



Published in final edited form as:

Nature. 2016 February 25; 530(7591): 485–489. doi:10.1038/nature16963.

Inhibiting Fungal Multidrug Resistance by Disrupting an Activator-Mediator Interaction

Joy L. Nishikawa^{1,2}, Andras Boeszoermyeni³, Luis A. Vale-Silva⁴, Riccardo Torelli⁵, Brunella Posteraro⁶, Yoo-Jin Sohn^{1,2}, Fei Ji^{7,8}, Vladimir Gelev⁹, Dominique Sanglard⁴, Maurizio Sanguinetti⁵, Ruslan I. Sadreyev^{7,10}, Goutam Mukherjee^{12,13}, Jayaram Bhyravabhotla^{12,13,14}, Sara J. Buhrlage^{3,11}, Nathanael S. Gray^{3,11}, Gerhard Wagner^{3,*}, Anders M. Näär^{1,2,*}, and Haribabu Arthanari^{3,*}

¹Massachusetts General Hospital Cancer Center, Charlestown, MA, USA ²Department of Cell Biology, Harvard Medical School, Boston, MA, USA ³Department of Biological Chemistry and Molecular Pharmacology, Harvard Medical School, Boston, MA, USA ⁴Institute of Microbiology, University Hospital Lausanne and University Hospital Center, Lausanne, Switzerland ⁵Institute of Microbiology, Università Cattolica del Sacro Cuore, Rome, Italy ⁶Institute of Public Health, Università Cattolica del Sacro Cuore, Rome, Italy ⁷Department of Molecular Biology, Massachusetts General Hospital, Boston, MA, USA ⁸Department of Genetics, Harvard Medical School, Boston, MA, USA ⁹Faculty of Chemistry and Pharmacy, Sofia University, Bulgaria ¹⁰Department of Pathology, Massachusetts General Hospital and Harvard Medical School, Boston, MA, USA ¹¹Dana-Farber Cancer Institute, Boston, MA, USA ¹²Department of Chemistry, Indian Institute of Technology Delhi, Hauz Khas, New Delhi-India ¹³Supercomputing Facility for Bioinformatics & Computational Biology, Indian Institute of Technology Delhi, Hauz Khas, New Delhi-India ¹⁴Kusuma School of Biological Sciences, Indian Institute of Technology Delhi, Hauz Khas, New Delhi-India

Eukaryotic transcription activators stimulate the expression of specific sets of target genes through recruitment of co-activators such as the RNA polymerase II-interacting Mediator complex^{1,2}. Aberrant function of transcription activators has been implicated in a number of diseases. However, therapeutic targeting efforts have been hampered by a lack of detailed molecular knowledge of the mechanisms of gene activation by disease-associated

Users may view, print, copy, and download text and data-mine the content in such documents, for the purposes of academic research, subject always to the full Conditions of use:http://www.nature.com/authors/editorial_policies/license.html#terms

*To whom correspondence should be addressed: G.W. (; Email: gerhard_wagner@hms.harvard.edu), A.M.N. (; Email: naar@helix.mgh.harvard.edu), H.A. (; Email: hari_arthanari@hms.harvard.edu)

Author Contributions

J.N., A.B., G.W., A.M.N., and H.A. conceived and designed the studies. A.B. and H.A. performed experiments relating to protein structure, small molecule screening and small molecule-protein interaction and data analysis. J.B. and G.M. performed the docking and free energy calculations. V.G., S.B. and N.G. designed the synthesis for *iKIX1* and its analogs. J.N. performed the *in vivo* small molecule screen, luciferase, ChIP, transcription, efflux, spot plating, combination index and mammalian cell culture (HepG2) experiments. Y.S. performed transcription and efflux experiments. J.N. prepared samples for RNA-Seq analysis; bioinformatic analysis was carried out by F.J. and R.S. L.V. and D.S. designed and performed moth survival and adhesion assays. R.T., B.P. and M.S. designed and executed mouse fungal burden and UTI model studies. J. N., A. B., G.W., A.M.N. and H.A. wrote the manuscript with input from the team.

Coordinates and NMR resonance assignments have been deposited in the Protein Data Bank (PDB code 4D7X) and Biological Magnetic Resonance Data Bank (BMRB code 25372).

transcription activators. We previously identified an activator-targeted three-helix bundle KIX domain in the human MED15 Mediator subunit that is structurally conserved in Gal11/Med15 Mediator subunits in fungi^{3,4}. The Gal11/Med15 KIX domain engages pleiotropic drug resistance transcription factor (Pdr1) orthologues, which are key regulators of the multidrug resistance (MDR) pathway in *S. cerevisiae* and in the clinically important human pathogen *Candida glabrata*^{5,6}. The prevalence of *C. glabrata* is rising, partly due to their low intrinsic susceptibility to azoles, the most widely used antifungal^{7,8}. Drug-resistant clinical isolates of *C. glabrata* most commonly harbour point mutations in Pdr1 that render it constitutively active⁹⁻¹⁴ suggesting that this transcriptional activation pathway represents a linchpin in *C. glabrata* MDR. We have carried out sequential biochemical and *in vivo* high-throughput screens to identify small molecule inhibitors of the interaction of the *C. glabrata* Pdr1 activation domain with the *C. glabrata* Gal11A KIX domain. The lead compound (*iKIX1*) inhibits Pdr1-dependent gene activation and re-sensitizes drug-resistant *C. glabrata* to azole antifungals *in vitro* and in animal models for disseminated and urinary tract *C. glabrata* infection. Determining the NMR structure of the *C. glabrata* Gal11A KIX domain provided a detailed understanding of the molecular mechanism of Pdr1 gene activation and MDR inhibition by *iKIX1*. We have demonstrated the feasibility of small molecule targeting of a transcription factor-binding site in Mediator as a novel therapeutic strategy in fungal infectious disease. Based on our previous findings that deletion of the KIX domain of *Saccharomyces cerevisiae* *GAL11* or *Candida glabrata* *GAL11A* abrogates Pdr1-dependent transcriptional responses and xenobiotic tolerance we hypothesized that the *CgPdr1-CgGal11A* interaction interface might serve as a promising target for novel anti-MDR compounds³. A fluorescently tagged *CgPdr1* activation domain (AD) was used in an *in vitro* fluorescence polarization (FP) screen¹⁵ of ~140,000 chemically diverse compounds to identify small molecules that block the interaction between the *CgGal11A* KIX domain and the *CgPdr1* AD (Extended Data Fig. 1). Based on the high degree of conservation between *S. cerevisiae* and *C. glabrata*, we followed up the top hits from the FP screen with an azole growth inhibition screen in *S. cerevisiae* to identify hits with *in vivo* efficacy (Fig. 1a). We identified 5 compounds that reproducibly inhibited growth in a concentration-dependent manner only in the presence of ketoconazole (Extended Data Fig. 1). The most potent compound is referred to as *iKIX1* (Fig. 1b, c). *In vitro* binding studies revealed that the Kd of the *CgPdr1* AD for the *CgGal11A* KIX domain is 0.32 μ M and the apparent Ki for *iKIX1* is 18 μ M (Fig. 1d).

To facilitate the elucidation of the mechanism of action of *iKIX1*, we determined the high-resolution solution structure of the *CgGal11A* KIX domain with a backbone RMSD of 0.7 Å (Fig. 2 and Extended Data Table 1; PDB # 4D7X). The *CgGal11A* KIX domain has 51% sequence identity and 61% similarity with the *S. cerevisiae* Gal11/Med15 KIX domain³ with an overall RMS deviation of 2.0 Å (Fig. 2a & Extended Data Fig. 2c). The *CgGal11A* KIX domain forms a three-helix bundle harbouring an extensively hydrophobic core and a short helix at the N-terminus (Fig. 2a). We determined interaction interfaces of the *CgGal11A* KIX domain with the *CgPdr1* AD and *iKIX1* (Fig. 2b) by chemical shift perturbation (CSP) analysis. The *CgPdr1* AD and *iKIX1* target the same large hydrophobic groove harboured by the three helices. Residues from all three helices constitute the interaction interface, and titration of an ILV-methyl labeled *CgGal11A* KIX domain reveals large CSPs on the three

leucines (L19, L23 and L51) upon addition of *CgPdr1* AD and *iKIX1* (Extended Data Fig. 2*b*). The basic interaction interface on the KIX domain complements the acidic residues of *CgPdr1* AD (Fig. 2*c*). Residues of the *CgGal11A* KIX domain that interact with *CgPdr1* AD and *iKIX1* overlap strongly, suggesting direct competitive binding as the mechanism of inhibition. Docking of *iKIX1* to the *CgGal11A* KIX domain suggests extensive hydrogen bonding and hydrophobic interactions between *iKIX1* and KIX domain residues (Fig. 2*d* and Extended Data Fig. 2*a*), matching the interaction interface mapped by CSP analysis.

To assess the *in vivo* effects of *iKIX1* on Pdr1-dependent transcription, we initially utilized a strain in which the two *S. cerevisiae* *PDR1* orthologues (*ScPDR1* and *ScPDR3*) are deleted and which carries a plasmid expressing *CgPDR1*³, and a heterologous luciferase gene driven by 3 pleiotropic drug response elements (PDREs). Luciferase activity was strongly induced by ketoconazole treatment; *iKIX1* co-treatment was able to block this induction in a concentration-dependent manner (Fig. 3*a*).

A chromatin immunoprecipitation (ChIP) assay was used to examine Gal11/Med15 recruitment to Pdr1-regulated target genes in *S. cerevisiae* after *iKIX1* treatment. Gal11/Med15 was rapidly recruited to the promoters of the Pdr1 target genes *PDR5* and *SNQ2* after ketoconazole addition; in contrast, ketoconazole-induced recruitment of Gal11/Med15 was abrogated when the cells were pre-treated with *iKIX1* (Fig. 3*b*, Extended Data Fig. 3*a*). *iKIX1* did not impede the constitutive occupancy of Pdr1 at the same Pdr1-regulated target genes (Extended Data Fig. 3*b*). Consistent with the ChIP data, *iKIX1* strongly inhibited azole-induced transcription of *ScPdr1* target genes (Fig. 3*c*, Extended Data Fig. 3*a*, *c*).

Next, we determined the effect of *iKIX1* on the transcription of *C. glabrata* Pdr1-regulated genes involved in drug efflux and MDR (*CgCDR1*, *CgCDR2* and *CgYOR1*). *CgPdr1* targets were strongly up-regulated after ketoconazole treatment^{12,16}. However, pre-treatment with *iKIX1* reduced target gene induction in a durable and concentration-dependent manner (Fig. 3*d* and Extended Data Fig. 4*a*, *b*). Treatment with *iKIX1* alone did not significantly affect Pdr1-target gene induction (Extended Data Fig. 4*c*, *d*).

Next generation RNA sequencing (RNA-Seq) was employed to query the genome-wide effects of *iKIX1* and azole treatments alone and in combination on the transcriptome in both *S. cerevisiae* and in *C. glabrata*. In accord with previous reports^{16,17}, azole treatment up-regulates Pdr1-dependent genes in both yeasts, such as the drug efflux pumps *ScPDR5* and *CgCDR1* (Supplementary Tables 1 and 2). Combined azole and *iKIX1* treatment strongly blunted expression of many azole-activated and Pdr1-dependent genes in both *S. cerevisiae* and *C. glabrata* (Fig. 3*e*, Extended Data Fig. 3*d* and Supplementary Tables 1 and 2), consistent with prior data and the proposed mechanism of action of *iKIX1*. *iKIX1* alone affected very different sets of genes in *S. cerevisiae* and *C. glabrata* (Supplementary Tables 1–3). Treatment of *S. cerevisiae* and *C. glabrata* cells with *iKIX1* did not significantly alter the expression of *PDR1* or *GAL11/MED15* after azole treatment (Extended Data Fig. 3*e*). Together, these findings suggest that the primary mechanism of synergistic antifungal effects of *iKIX1* with azoles is through blocking the azole-stimulated and Pdr1-dependent drug efflux pathway.

To ascertain *iKIX1* efficacy in azole-resistant *C. glabrata* strains, we examined the effects of *iKIX1* on *CgPdr1* target gene expression in a set of isogenic strains with gain-of-function *CgPDR1* mutations originally identified in azole-resistant *C. glabrata* clinical isolates⁹. *iKIX1* reduced azole-induced transcription of *CgPdr1* target genes (e.g., *CgCDR1*) in a concentration-dependent manner in all strains tested (Fig. 3*f* and Extended Data Fig. 4*d*).

To investigate whether these transcriptional effects translated to functional effects on drug efflux rates, we utilized the fluorescent compound rhodamine 6G, a substrate of the *CgCdr1* efflux pump^{18,19}. Maximum efflux rates were significantly decreased in *PDR1* wild-type or gain-of-function strains pre-treated with *iKIX1*, as compared to vehicle control (Fig. 3*g* and Extended Data Fig. 5).

Due to its ability to reduce efflux pump gene expression and pump activity, we predicted that *iKIX1* could restore azole-sensitivity to *CgPDR1* gain-of-function mutant strains. Isogenic *C. glabrata* strains with wild-type or single gain-of-function alterations across *CgPdr1* (Fig. 4*a*) were tested for their sensitivity to fluconazole or ketoconazole on gradient plates with increasing concentrations of *iKIX1* or vehicle. As expected, a *CgPDR1* wild-type strain was sensitive to both fluconazole and ketoconazole, whereas *CgPDR1* gain-of-function mutant strains grew robustly in the presence of azoles. *iKIX1* restored azole-sensitivity to *PDR1* gain-of-function mutant strains in a concentration-dependent manner (Fig. 4*b*). *CgPDR1* wild-type strains also exhibited increased growth inhibition in the presence of both *iKIX1* and azole versus single agents alone (Extended Data Fig. 6*a, b*).

Based on the strong combination effect of azoles and *iKIX1* in the *CgPDR1*^{L280F} mutant we focused follow-up studies on this mutant strain. To investigate whether azoles and *iKIX1* act in a synergistic or additive manner in *CgPDR1* wild-type and *CgPDR1*^{L280F} mutant strains, we assessed growth in checkerboard assays with ketoconazole and *iKIX1*. In the wild-type *CgPDR1* strain, the combination of ketoconazole and *iKIX1* was additive (Extended Data Fig. 6*c*). However, the *CgPDR1*^{L280F} mutant exhibited synergistic growth inhibition with *iKIX1* and ketoconazole combination treatment, with combination indices <1 (Extended Data Fig. 6*d*), in concordance with the spot-plating assay.

We carried out a limited analysis exploring the chemical space around the *iKIX1* scaffold using commercial and custom synthesized *iKIX1* analogs, identifying several compounds that lost activity in all assays; one analog (A2) is shown in Extended Data Figure 7*a–d*. This example, together with data from *iKIX1* analogs and the docked structure of *iKIX1* to the *CgGal11A* KIX domain, supports a model where *iKIX1* engages the core of the KIX domain using an array of hydrophobic and hydrogen bond contacts.

We utilized two metazoan model systems to evaluate the potential utility of *iKIX1* as a co-therapeutic with fluconazole to treat disseminated *C. glabrata* infection. The larvae of the moth *Galleria mellonella* has been used as a model to test the pathogenicity of a wide variety of human pathogens²⁰. We utilized a *G. mellonella* survival assay to determine the virulence of *C. glabrata* *PDR1* wild-type or *PDR1*^{L280F} strains in the presence of fluconazole, *iKIX1*, or a combination of the two (Fig. 4*c*). Larvae were injected with *C. glabrata* and a single injection of fluconazole (50 mg/kg), *iKIX1* (25 mg/kg), a combination of the two, or

vehicle; survival was monitored every 24 hours. *G. mellonella* injected with wild-type *CgPDR1* was sensitive to fluconazole alone, and exhibited no significant alterations in survival with a fluconazole-*iKIX1* combination. However, in *G. mellonella* larvae injected with a *CgPDR1^{L280F}* strain, whereas the single agents fluconazole or *iKIX1* did not significantly increase survival compared to vehicle, co-treatment with *iKIX1* and fluconazole significantly increased survival ($P < 0.001$).

Prior to mammalian studies, we sought to evaluate the potential toxicity of *iKIX1* in mammalian cells (Extended Data Fig. 7e, f). Human HepG2 cells treated with *iKIX1* revealed toxicity only at high concentrations of *iKIX1* ($IC_{50} \sim 100 \mu M$). *iKIX1* had no effect on the transcription of SREBP-target genes at concentrations up to $100 \mu M$, indicating its specificity for the fungal Gal11/Med15 KIX domain⁴. We also assessed the *in vitro* stability and *in vivo* mouse pharmacokinetics of *iKIX1* and found that *iKIX1* exhibited favorable drug-like properties and *in vivo* exposure in these studies (Extended Data Fig. 8g,h).

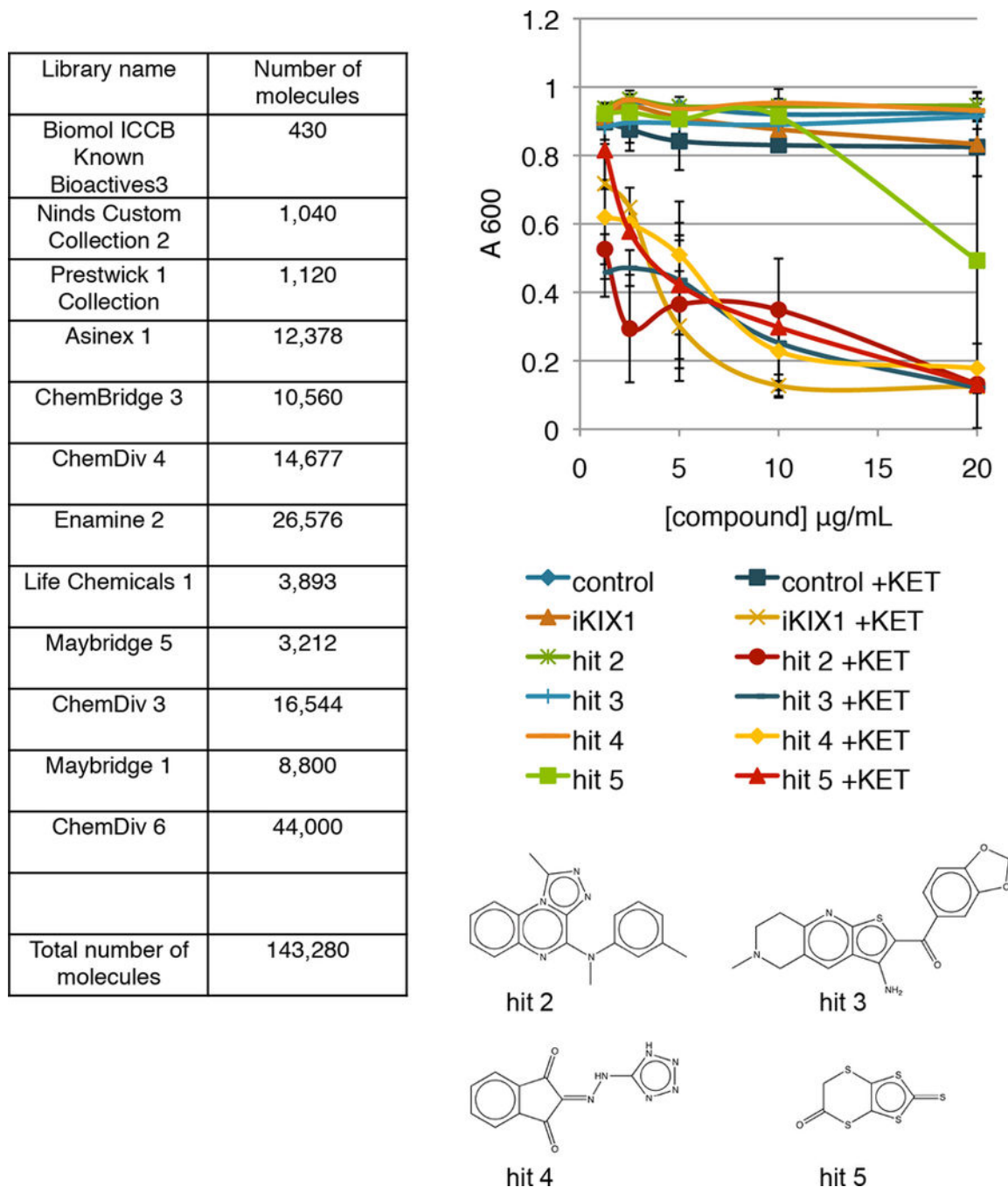
To evaluate the therapeutic potential of *iKIX1* and azole antifungal co-therapy in a mammalian model, we initially turned to an established mouse model of disseminated fungal disease¹¹. Mice were inoculated with *C. glabrata* by tail-vein injection and were dosed peritoneally once-daily with 100 mg/kg fluconazole (high FLU), 100 mg/kg *iKIX1*, a combination of the two, or vehicle alone. After 7 days, mice injected with a *CgPDR1* wild-type strain exhibited significantly reduced tissue fungal burden in the kidney and spleen following fluconazole treatment alone; *iKIX1* co-treatment did not result in further reductions (Fig. 4d). In contrast, in mice injected with the azole-resistant *CgPDR1^{L280F}* strain, only co-treatment with *iKIX1* and fluconazole resulted in significant (~ 10 -fold) reductions in fungal burdens in the kidney and spleen ($P < 0.0001$) (Fig. 4d). Similar results were observed with the clinically isolated *CgPDR1⁺* and *CgPDR1^{L280F}* strains DSY562 and DSY565 (Extended Data Fig. 8a). Consistent with previous studies⁹, the fungal burden in mice infected with the *CgPDR1^{L280F}* strain was higher than those infected with wild-type *CgPDR1* strains, suggesting that *PDR1* mutant strains may be more virulent *in vivo*. Similar but less pronounced results were found in mice injected with a *CgPDR1^{P822L}* strain (Extended Data Fig. 8b). When mice were injected with a *CgPDR1* wild-type strain and dosed with 25 mg/kg fluconazole (low FLU) alone or in combination with *iKIX1*, fluconazole alone poorly reduced tissue burden, whereas combination treatment resulted in significant (~ 10 -fold) reductions in fungal burdens in both organs ($P < 0.0001$) (Fig. 4d). These results suggest that *iKIX1* combination treatment with azole may be therapeutically desirable even in the absence of *CgPDR1* gain-of-function mutations. Mice infected with a *Cgpd1* null strain were more sensitive to *iKIX1* alone; unlike mice infected with *CgPDR1⁺* or *CgPDR1^{L280F}* strains, low doses of *iKIX1* did not further reduce fungal burden in *Cgpd1* null infections (Extended Data Fig. 8c,d).

CgPDR1 gain-of-function mutations are also known to control adherence to host cells. As previously observed²¹, a *PDR1^{L280F}* mutant increased relative adherence to epithelial cells as compared to a *PDR1* wild-type strain. Strikingly, *iKIX1* treatment alone reduced adherence to levels similar to a *PDR1* wild-type strain (Extended Data Fig. 8e). Ketoconazole alone or co-treatment with *iKIX1* also reduced relative adherence to levels comparable to a *PDR1* wild-type strain. To assess the role of *iKIX1* in modulating adhesion

in an infection model, we turned to a mouse model of urinary tract infection²². In both the bladder and kidney, *iKIX1* alone was sufficient to decrease fungal load after infection with either a *PDR1* wild-type strain or a *PDR1*^{L280F} strain (Extended Data Fig. 8f), suggesting that *iKIX1* may indeed modulate adhesion.

The proportion of azole-resistant *C. glabrata* (up to 20% in the US) and the emergence of multidrug resistance (approximately 40% of echinocandin-resistant isolates are azole-resistant) argues for the need for novel treatments that can target these resistant populations^{23,24}. Our results demonstrate that small molecule disruption of the interaction between the *CgGal11A* KIX domain and the *CgPdr1* activation domain is a therapeutically tractable method for resensitizing azole-resistant *C. glabrata* to standard azole antifungal treatment (Extended Data Fig. 9).

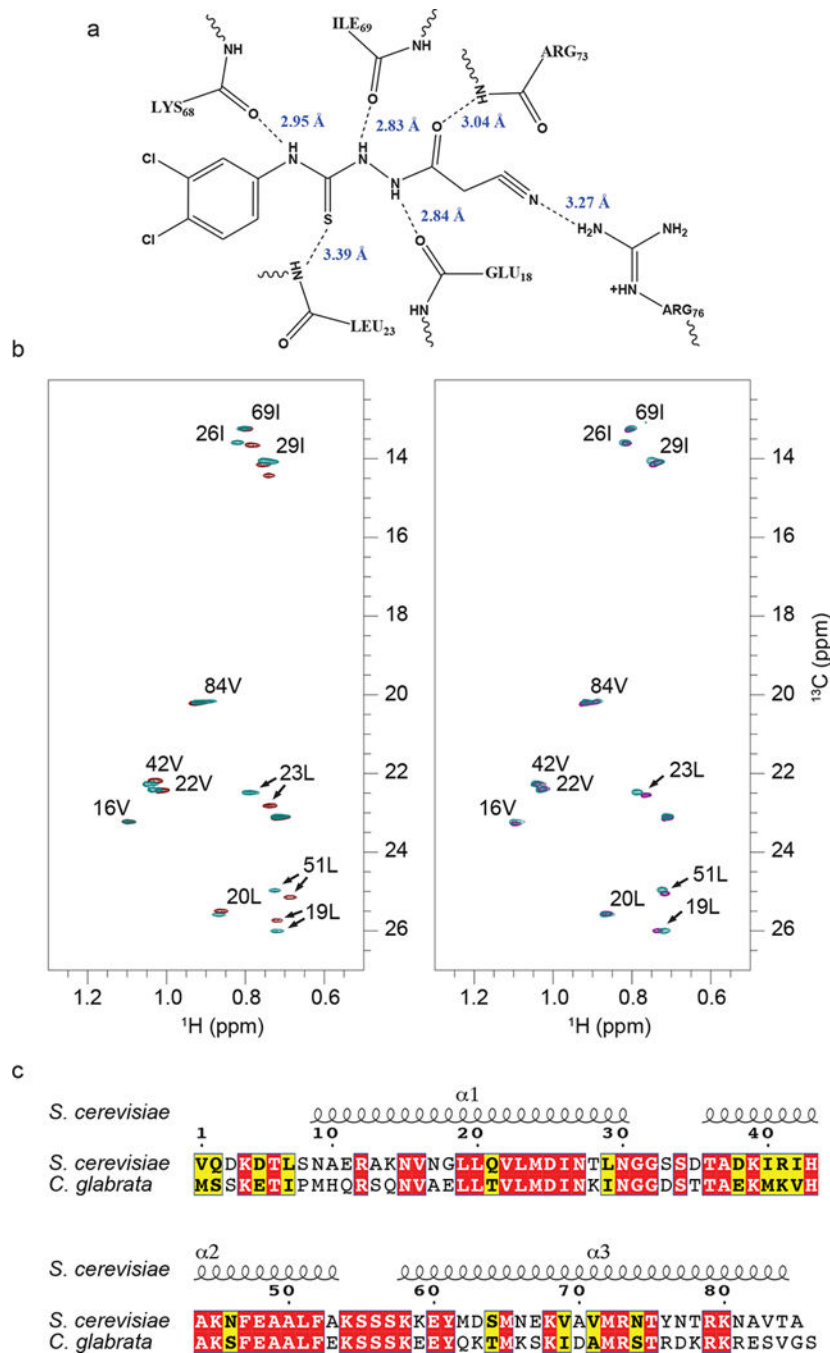
Extended Data

**Extended Data Figure 1.**

Left: Table of compound libraries that were screened using a fluorescence polarization assay at the Institute of Chemistry & Cell Biology (ICCB) facility at Harvard Medical School.

Right: An *S. cerevisiae* viability screen identifies small molecules that preferentially inhibit growth of *S. cerevisiae* in a concentration-dependent manner in the presence of 5 μ M

ketoconazole (KET). Top hits from the screen are shown; OD₆₀₀ values are the average of values from duplicate plates.

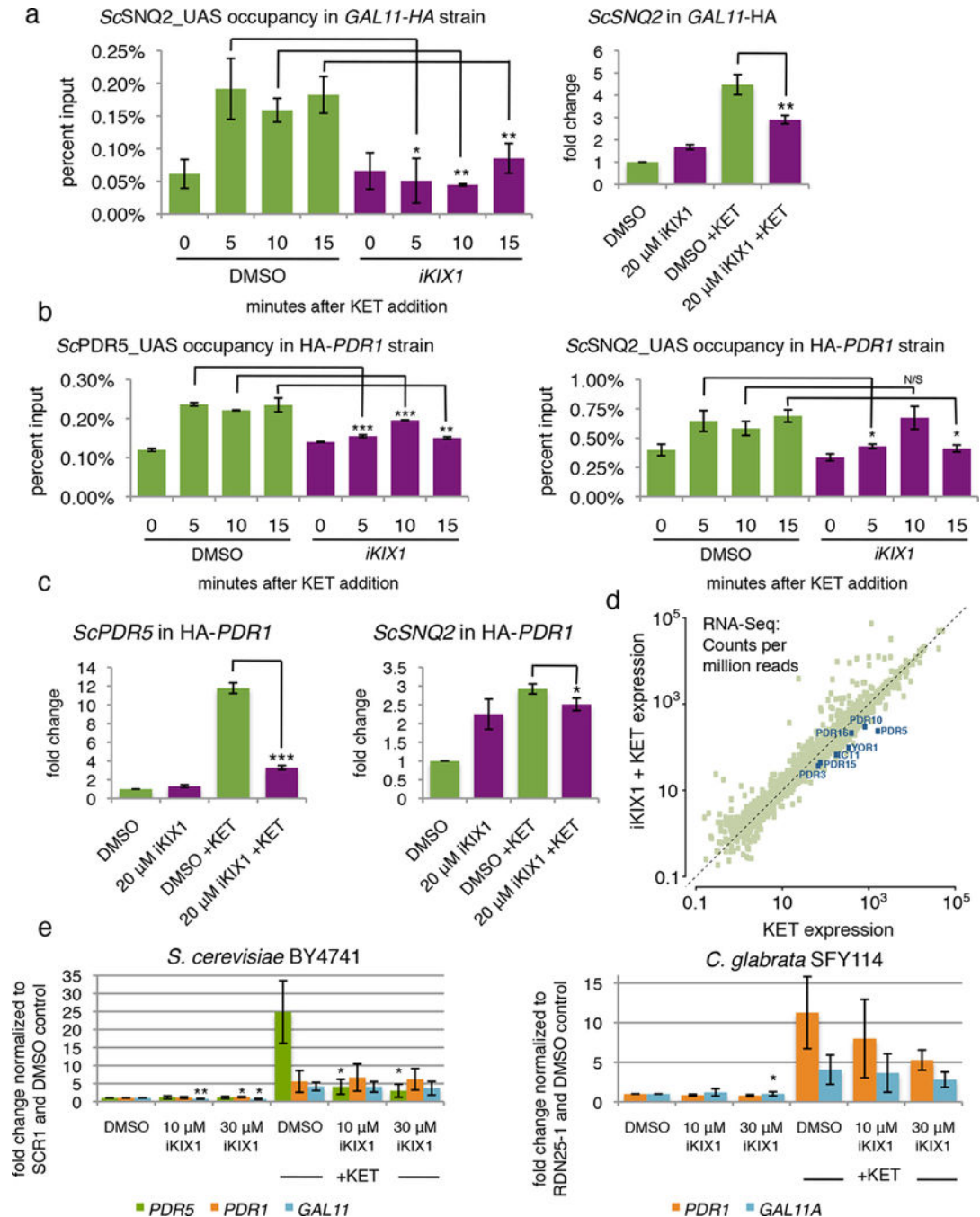


Extended Data Figure 2.

(a) 2-dimensional representation of the H-bonding network between the *CgGal11A* KIX domain and *iKIXI* based on docking studies.

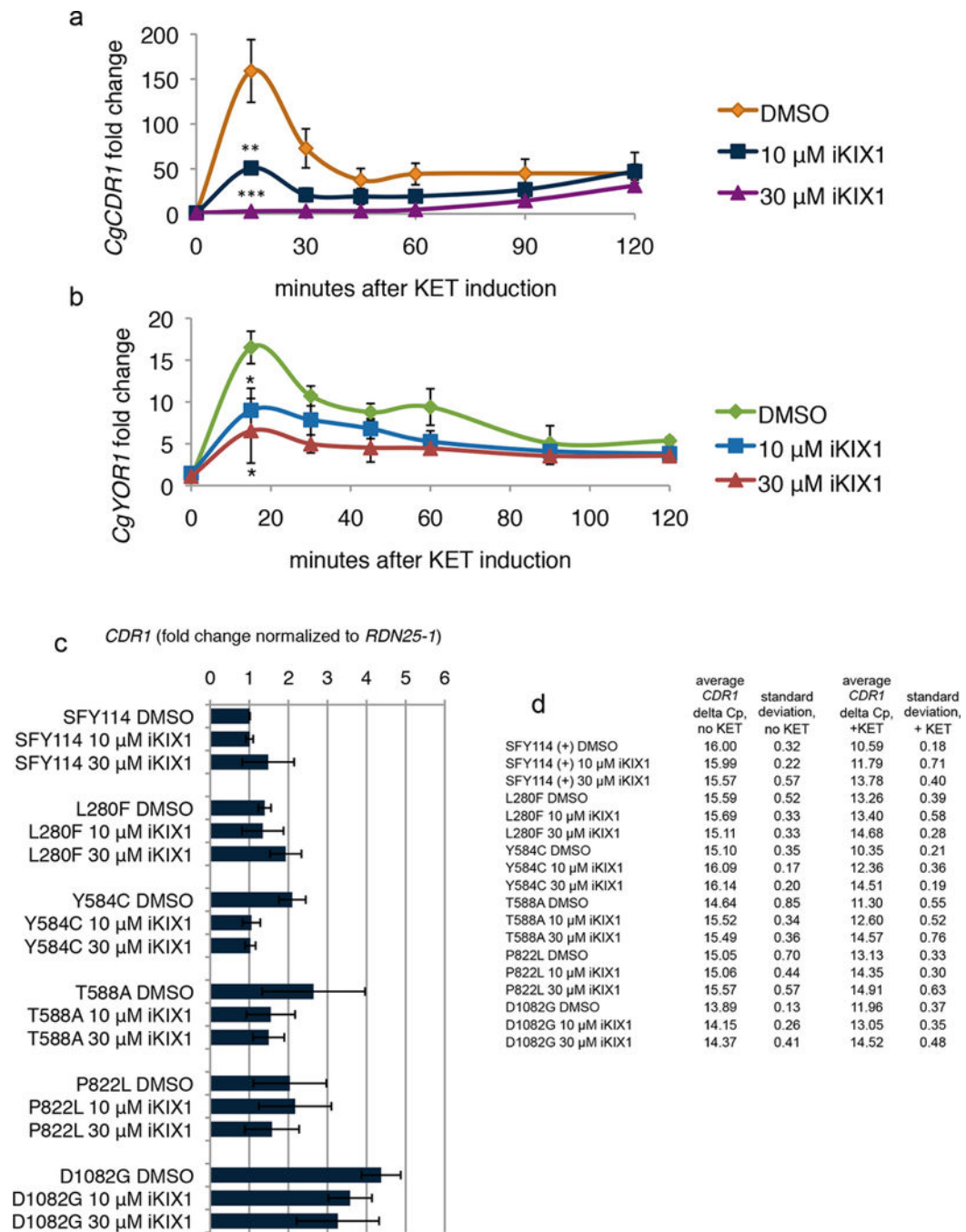
(b) Chemical shift perturbations (CSPs) of ILV methyl resonances. Left: ¹H-¹³C HSQC showing ILV methyl resonances of *CgGal11A* KIX domain in presence (brown) and absence

(teal) of *CgPdr1* AD (2-fold excess). Right: ^1H - ^{13}C HSQC showing ILV methyl resonances of *CgGal11A* KIX domain in presence (purple) and in absence (teal) of *iKIX1* (4-fold excess). Three leucines (L19, L23, L51) show significant CSPs in both spectra. (c) Sequence alignment of the *C. glabrata* Gal11A and *S. cerevisiae* Gal11/Med15 KIX domains²⁶.



Extended Data Figure 3.

- (a) *iKIX1* prevents the ketoconazole (KET)-induced recruitment of *ScGal11/Med15/* Mediator to the upstream activating sequences (UAS) of the PDRE-regulated promoter *ScSNQ2* and transcriptional upregulation of *ScSNQ2*.
- (b) HA-Pdr1 occupies PDRE-regulated promoters of *ScPDR5* and *ScSNQ2* in the presence of 20 μ M *iKIX1* or vehicle (DMSO) control prior to and following ketoconazole (KET) addition.
- (c) 20 μ M *iKIX1* inhibits ketoconazole-induced upregulation of *ScPdr1* target genes *ScPDR5* and *ScSNQ2* in the HA-Pdr1 strain. RNA was harvested concurrently with representative chromatin immunoprecipitation experiment shown in panel (b) at t=0 min. (DMSO, 20 μ M *iKIX1*) and t=15 min. after ketoconazole induction (DMSO + KET, 20 μ M *iKIX1* + KET). Transcripts are normalized to *ScSCR1* and un-induced DMSO control. (a–c) Representative experiment from two biological replicates is shown. Error bars represent mean \pm s.d. of technical replicates; *P<0.05, **P<0.01 and ***P<0.001 as calculated by two-tailed Student's t-test.
- (d) RNA-Seq analysis of a wild-type *S. cerevisiae* strain (BY4741) pre-treated with *iKIX1* or vehicle alone then induced with ketoconazole (*iKIX1* + KET and KET, respectively) demonstrate a blunted induction of Pdr1 target genes following *iKIX1* pre-treatment. Data represents means of three biological replicates.
- (e) *iKIX1* pre-treatment does not significantly alter the transcript levels of *PDR1* or *GAL11/ GAL11A* in *S. cerevisiae* or *C. glabrata* after azole induction. Cells were pre-incubated with vehicle (DMSO) or *iKIX1* and then induced with 40 μ M ketoconazole (+KET) for 15 minutes before harvest. Average value of three biological replicates is shown and error bars represent mean \pm standard deviation; * P<0.05, ** P<0.001 as compared to DMSO or DMSO+KET control, calculated by two-tailed Student's t-test.

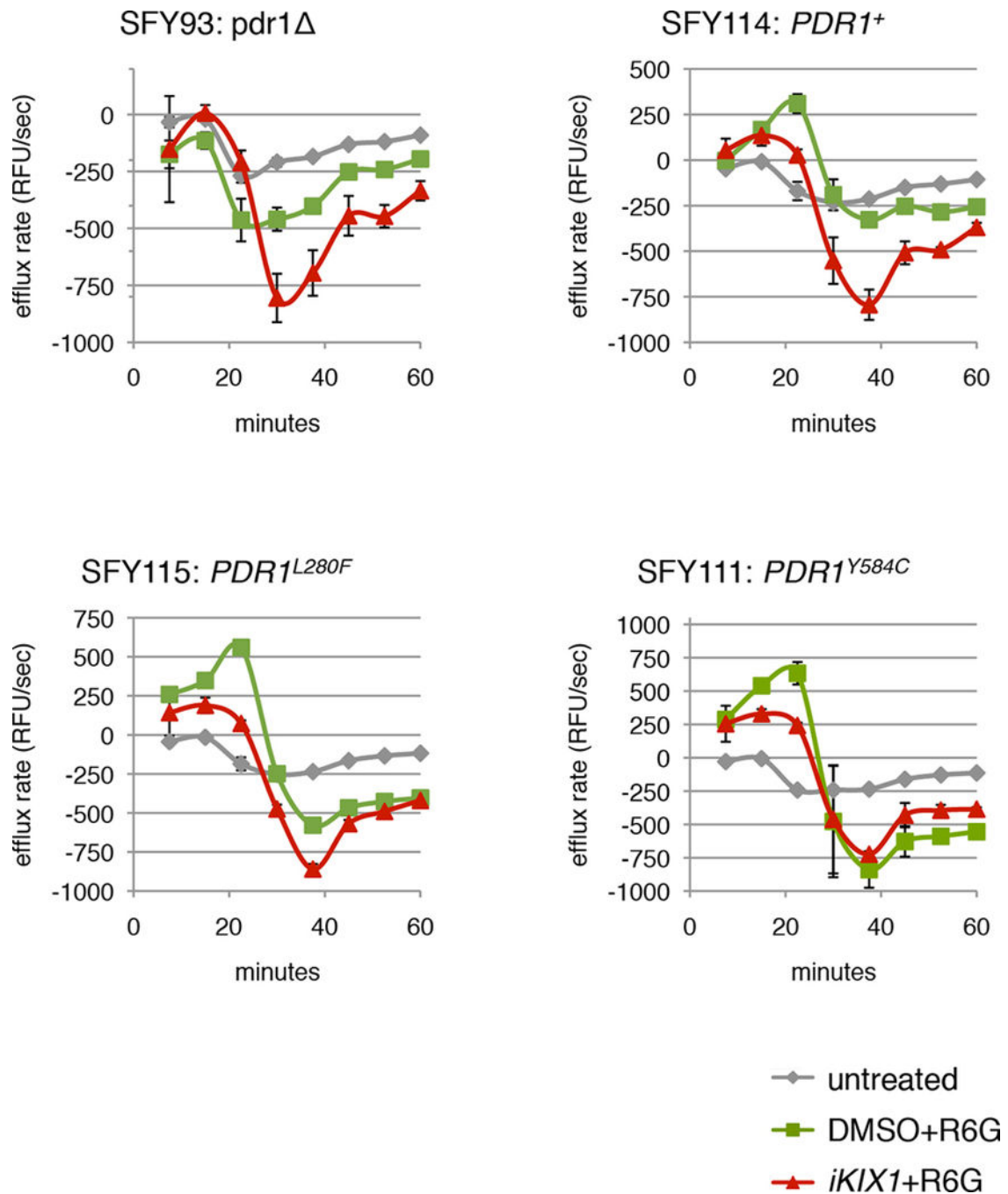
**Extended Data Figure 4.**

With *iKIX1* pre-treatment, *CgPdr1*-dependent transcription of (a) *CgCDR1* and (b) *CgYOR1* remains repressed 120 minutes after ketoconazole induction. SFY114 (*PDR1* wild-type) cells were pre-incubated with vehicle (DMSO) or *iKIX1* and then induced with 40 μ M ketoconazole (+KET). Transcript levels were assessed by quantitative RT-PCR prior to and for 120 minutes following ketoconazole induction. Transcript levels are normalized to *CgRDN25-1* and un-induced vehicle control (DMSO) at $t=0$.

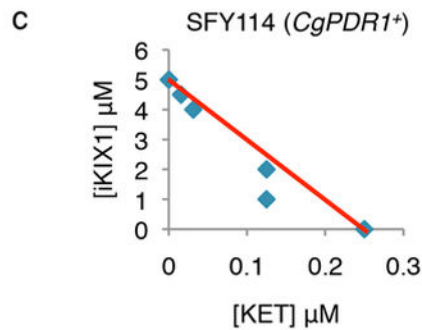
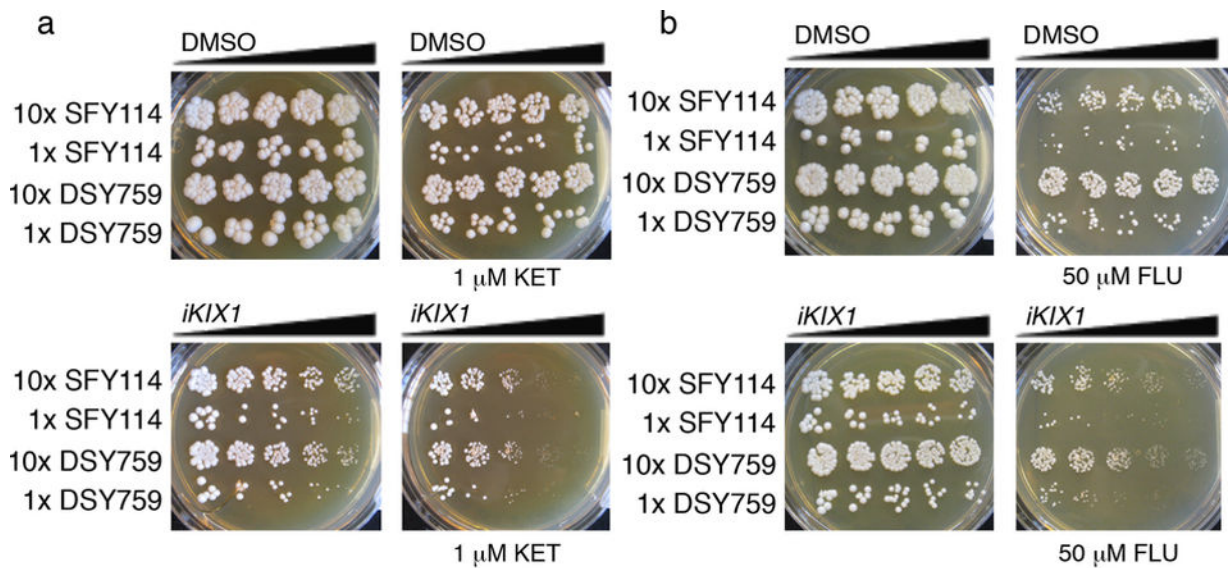
(c) *iKIX1* treatment alone does not have significant effects on *CgPdr1* target gene induction either in the presence of wild-type (SFY114) or gain-of-function mutant *CgPDR1* (amino acid alterations indicated).

(d) Table of average *CgCDR1* delta Cp values ($Cp_{CgCDR1} - Cp_{CgRDN25-1}$) and corresponding standard deviation for quantitative real-time PCR experiments shown in Figure 3f and Extended Data Figure 4c.

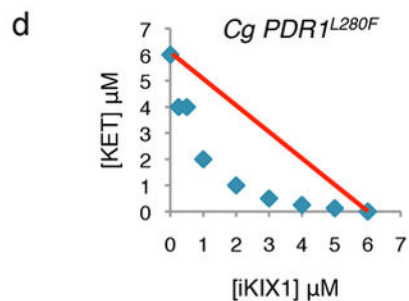
(a–d) For all panels of Extended Data Figure 4, average value of three biological replicates is shown and error bars represent \pm standard deviation; * $P < 0.05$, ** $p < 0.01$, and *** $p < 0.005$ as compared to vehicle + ketoconazole control. P values calculated using two-tailed Student's t-test.

**Extended Data Figure 5.**

iKIX1 inhibits efflux of rhodamine 6G in *PDR1* wild-type, *PDR1*^{L280F} and *PDR1*^{Y584C} strains. Data points indicate mean of three biological replicates and error bars represent mean \pm s.d.



IC ₅₀ KET (μM)	IC ₅₀ <i>iKIX1</i> (μM)	CI
0	5	1.00
0.015625	4.5	0.96
0.03125	4	0.93
0.125	2	0.90
0.125	1	0.70
0.25	0	1.00



IC ₅₀ KET (μM)	IC ₅₀ <i>iKIX1</i> (μM)	CI
-	6	N/A
0.125	5	0.85
0.25	4	0.71
0.5	3	0.58
1	2	0.50
2	1	0.50
4	0.5	0.75
4	0.25	0.71
6	-	N/A

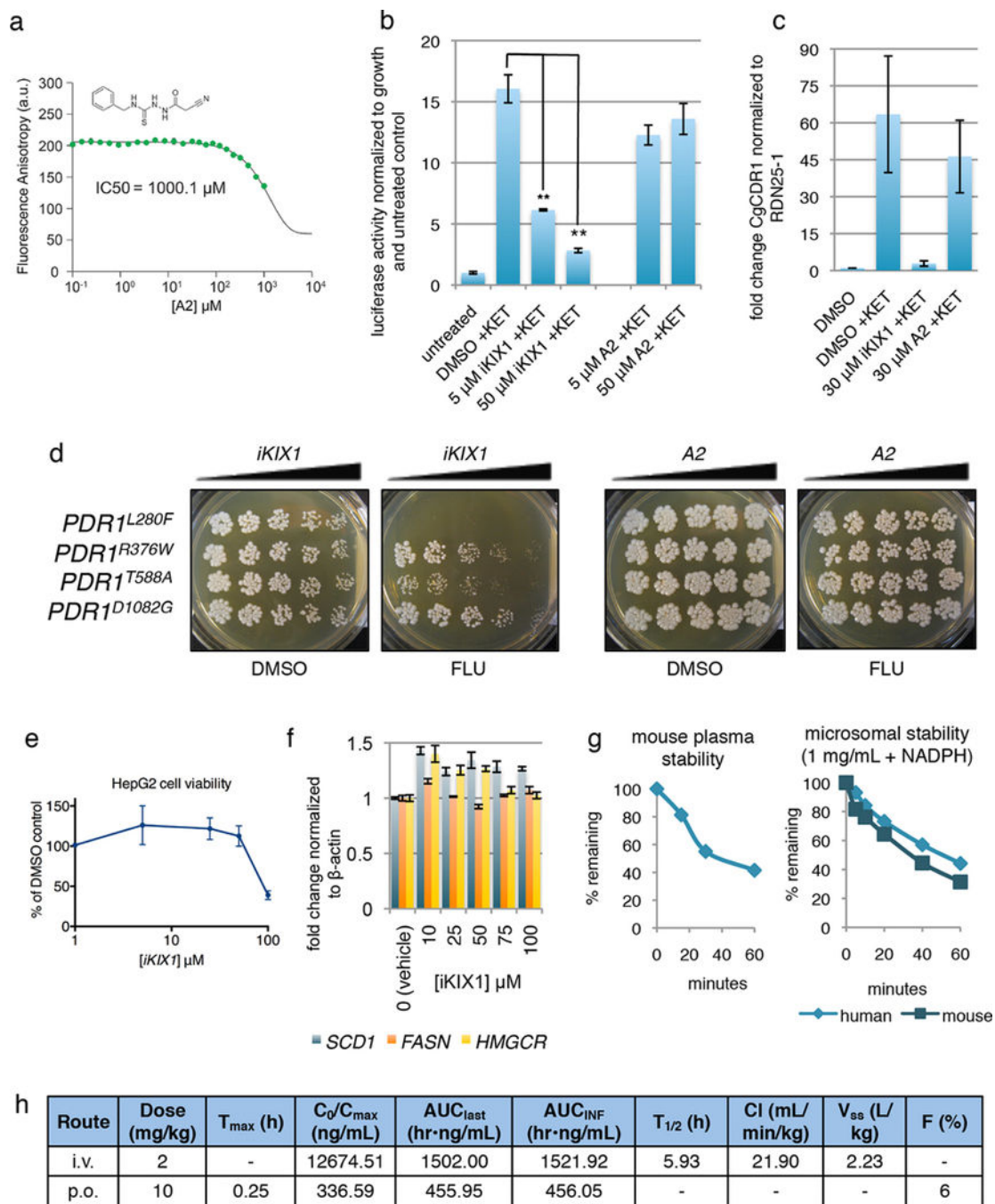
Extended Data Figure 6.

(a,b) *iKIX1* increases the sensitivity of *Cg* strains bearing wild-type *CgPDR1* to azole treatment. Two strains bearing wild-type *CgPDR1* alleles (SFY114, DSY759) were plated at concentrations differing by ten-fold (10×, 1×) on plates containing increasing concentrations of (a) *iKIX1* to 300 μM in the presence or absence of 1 μM ketoconazole (KETO) or (b) *iKIX1* to 250 μM in the presence or absence of 50 μM fluconazole (FLU).

(c) *iKIX1* and ketoconazole (KET) have additive effects on the growth of a *CgPDR1* wild-type strain.

(d) *iKIX1* and ketoconazole (KET) synergistically inhibit the growth of the *CgPDR1^{L280F}* mutant.

(c,d) The EUCAST broth microdilution method²⁷ was used to assess the effects of *iKIX1* and ketoconazole combination treatment. Growth, as assessed by OD₅₄₀, was normalized to no drug control. All combination indices (CI) for the *CgPDR1^{L280F}* mutant were less than 1, indicating synergy. A representative of three biological replicates is shown and the red line indicates a combination index of 1.



Extended Data Figure 7.

Electron-withdrawing groups in the aromatic ring of *iKIX1* complement the basic binding interface of the *CgGal11A* KIX domain and thus play a key role in *iKIX1* function.

A structurally similar *iKIX1* analog (*A2*) lacking electron-withdrawing groups increases the IC_{50} in the FP assay (a) and abolishes activity in the *S. cerevisiae* luciferase reporter assay (b), repression of *CgCDR1* expression (c), and synergistic *C. glabrata* cell growth inhibition with azoles (d).

Error bars in (b,c) indicate mean \pm s.d. of technical replicates (reads/real-time PCR reactions, respectively). ** $P < 0.005$; statistical differences calculated using two-tailed Student's t-test.

(e) *iKIX1* inhibits viability of HepG2 cells at concentrations $>50 \mu\text{M}$. The mean of 3 biological replicates is shown; error bars represent means \pm s.d.

(f) *iKIX1* exhibits no effect on transcription of SREBP-target genes in HepG2 cells at concentrations up to $100 \mu\text{M}$. Biological duplicates were assessed; representative experiment is shown and error bars represent means \pm s.d. of technical (real-time PCR) replicates.

(g) Mouse plasma stability of *iKIX1* and mouse and human microsomal stability of *iKIX1*, $n=1$

(h) *In vivo* pharmacokinetic parameters of *iKIX1*, $n=3$ mice per time point.

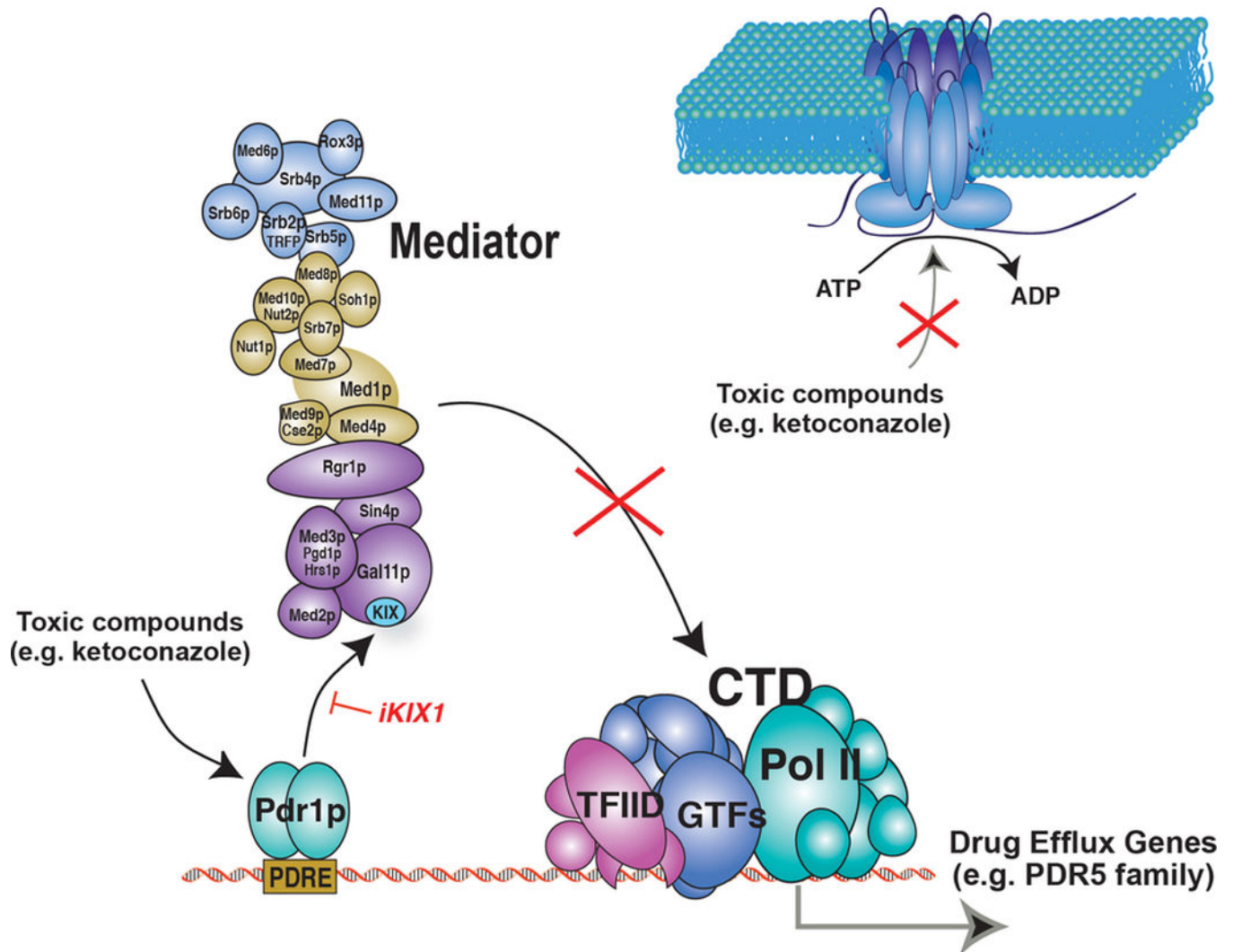
(c) 100 mg/kg/day *iKIX1* (high *iKIX1*) treatment of mice infected with SFY93 (*pdrl*⁻) significantly reduces fungal burden in a mouse infection model (CFU/g kidney) alone as compared to SFY114 (*PDR1*⁺) or SFY115 (*PDR1*^{L280F}). n=10 mice for each treatment condition; * P<0.01, ** P<0.005, *** P<0.0001.

(d) Mice infected with SFY114 (*PDR1*⁺), SFY115 (*PDR1*^{L280F}) or SFY93 (*pdrl*⁻) were treated with low (10 mg/kg/day) *iKIX1*, low fluconazole (low FLU; 25 mg/kg/day), fluconazole at 100 mg/kg/day (FLU) or combination with the two. *iKIX1* did not confer additional reductions in CFU/g kidney with SFY93 infection. n=10 mice for each treatment condition. *** P<0.0005.

(e) *iKIX1* and ketoconazole (KETO) reduce adherence of *CgPDR1*^{L280F} (SFY116) to CHO-Lec2 cells. Adherence is normalized to SFY114 DMSO control; each column represents the average of 4 biological replicates. * P<0.05 as compared to SFY114 DMSO control.

(f) *iKIX1* (100 mg/kg/day) or fluconazole (FLU) significantly reduces fungal burden in the bladder and kidney in a urinary tract infection model in mice. n=15 mice were infected in each group and points at 0 log₁₀ CFU/g organ fell below the detection limit of the method (50 CFU/g organ). * P< 0.05, ** P<0.005

(a–f) Statistical differences were measured using a Mann-Whitney/Wilcoxon rank-sum test as compared to no treatment control; error bars represent means +/- standard deviation.

**Extended Data Figure 9.**

Model of *iKIX1* function as a co-therapeutic in combination with an azole, blocking the azole-induced recruitment of Gal11/Med15-Mediator to Pdr1 target genes upon azole-treatment and preventing the upregulation of Pdr1 target genes, including those which encode drug efflux pumps.

Extended Data Table 1
NMR and refinement statistics for *CgGal11A* KIX domain

Summary of quality statistics for the ensemble of 10 structures calculated with AMBER explicit water refinement and list of experimental restraints.

Protein
NMR distance and dihedral constraints
Distance constraints

	Protein
Total NOE	1718
Intra-residue	602
Inter-residue	1116
Sequential ($ i-j = 1$)	517
Medium-range ($ i-j \leq 4$)	488
Long-range ($ i-j \geq 5$)	111
Hydrogen bonds	0
Total dihedral angle restraints	158
phi	79
psi	79
Structure statistics	
Violations (mean and s.d.)	
Distance constraints (Å)	0.083 ± 0.039
Dihedral angle constraints (°)	2.407 ± 0.357
Max. dihedral angle violation (°)	10.267
Max. distance constraint violation (Å)	0.248
Deviations from idealized geometry	
Bond lengths (Å)	0.013
Bond angles (°)	1.9
Average pairwise r.m.s.d. ^{**} (Å)	
Heavy	1.1
Backbone	0.7

^{**} Pairwise r.m.s.d. was calculated among ordered residues (3–83) of 10 refined structures.

Supplementary Material

Refer to Web version on PubMed Central for supplementary material.

Acknowledgments

We are grateful to Paul Coote, Evangelos Papadopoulos and Rafael Luna for helpful discussions and advice with data analysis and manuscript preparation. We acknowledge the ICCB-Longwood Screening Facility at Harvard Medical School for assistance with the high-throughput screens and access to the compound libraries, and the MGH Next Gen sequencing core for RNA-Seq library construction. Mouse plasma and microsomal stability experiments were carried out at the Scripps Research Institute and *iKIXI* pharmacokinetic parameters were assessed by Sai Life Sciences Limited. We acknowledge support from the National Institute of Health (grants GM047467 to G.W and A.M.N and EB002026 to G.W). J.N. was supported by an NSERC fellowship.

References

1. Conaway RC, Conaway JW. Function and regulation of the Mediator complex. *Current opinion in genetics & development*. 2011; 21:225–230. [PubMed: 21330129]
2. Poss ZC, Ebmeier CC, Taatjes DJ. The Mediator complex and transcription regulation. *Critical reviews in biochemistry and molecular biology*. 2013; 48:575–608. [PubMed: 24088064]
3. Thakur JK, et al. A nuclear receptor-like pathway regulating multidrug resistance in fungi. *Nature*. 2008; 452:604–609. [PubMed: 18385733]
4. Yang F, et al. An ARC/Mediator subunit required for SREBP control of cholesterol and lipid homeostasis. *Nature*. 2006; 442:700–704. [PubMed: 16799563]

5. Paul S, Moye-Rowley WS. Multidrug resistance in fungi: regulation of transporter-encoding gene expression. *Frontiers in physiology*. 2014; 5:143. [PubMed: 24795641]
6. Prasad R, Goffeau A. Yeast ATP-binding cassette transporters conferring multidrug resistance. *Annual review of microbiology*. 2012; 66:39–63.
7. Pfaller MA, et al. Variation in susceptibility of bloodstream isolates of *Candida glabrata* to fluconazole according to patient age and geographic location in the United States in 2001 to 2007. *J Clin Microbiol*. 2009; 47:3185–3190. doi:JCM.00946-09 [pii] 10.1128/JCM.00946-09. [PubMed: 19656983]
8. Pfaller MA, Messer SA, Moet GJ, Jones RN, Castanheira M. *Candida* bloodstream infections: comparison of species distribution and resistance to echinocandin and azole antifungal agents in Intensive Care Unit (ICU) and non-ICU settings in the SENTRY Antimicrobial Surveillance Program (2008–2009). *Int J Antimicrob Agents*. 38:65–69. doi:S0924-8579(11)00132-4 [pii] 10.1016/j.ijantimicag.2011.02.016. [PubMed: 21514797]
9. Ferrari S, et al. Gain of function mutations in CgPDR1 of *Candida glabrata* not only mediate antifungal resistance but also enhance virulence. *PLoS Pathog*. 2009; 5:e1000268. [PubMed: 19148266]
10. Ferrari S, Sanguinetti M, Torelli R, Posteraro B, Sanglard D. Contribution of CgPDR1-regulated genes in enhanced virulence of azole-resistant *Candida glabrata*. *PloS one*. 2011; 6:e17589. [PubMed: 21408004]
11. Silva LV, et al. Milbemycins: more than efflux inhibitors for fungal pathogens. *Antimicrobial agents and chemotherapy*. 2013; 57:873–886. [PubMed: 23208712]
12. Vermitsky JP, et al. Pdr1 regulates multidrug resistance in *Candida glabrata*: gene disruption and genome-wide expression studies. *Mol Microbiol*. 2006; 61:704–722. [PubMed: 16803598]
13. Sanguinetti M, et al. Mechanisms of azole resistance in clinical isolates of *Candida glabrata* collected during a hospital survey of antifungal resistance. *Antimicrob Agents Chemother*. 2005; 49:668–679. doi:49/2/668 [pii] 10.1128/AAC.49.2.668-679.2005. [PubMed: 15673750]
14. Caudle KE, et al. Genomewide expression profile analysis of the *Candida glabrata* Pdr1 regulon. *Eukaryot Cell*. 10:373–383. doi:EC.00073-10 [pii] 10.1128/EC.00073-10. [PubMed: 21193550]
15. Roehrl MH, Wang JY, Wagner G. A general framework for development and data analysis of competitive high-throughput screens for small-molecule inhibitors of protein-protein interactions by fluorescence polarization. *Biochemistry*. 2004; 43:16056–16066. [PubMed: 15610000]
16. Ferrari S, Sanguinetti M, Torelli R, Posteraro B, Sanglard D. Contribution of CgPDR1-regulated genes in enhanced virulence of azole-resistant *Candida glabrata*. *PLoS One*. 6:e17589. [PubMed: 21408004]
17. DeRisi J, et al. Genome microarray analysis of transcriptional activation in multidrug resistance yeast mutants. *FEBS Lett*. 2000; 470:156–160. doi:S0014-5793(00)01294-1 [pii]. [PubMed: 10734226]
18. Sanglard D, Ischer F, Calabrese D, Majcherczyk PA, Bille J. The ATP binding cassette transporter gene CgCDR1 from *Candida glabrata* is involved in the resistance of clinical isolates to azole antifungal agents. *Antimicrobial agents and chemotherapy*. 1999; 43:2753–2765. [PubMed: 10543759]
19. Silva LV, et al. Milbemycins: more than efflux inhibitors for fungal pathogens. *Antimicrob Agents Chemother*. 57:873–886. doi:AAC.02040-12 [pii] 10.1128/AAC.02040-12. [PubMed: 23208712]
20. Arvanitis M, Glavis-Bloom J, Mylonakis E. Invertebrate models of fungal infection. *Biochimica et biophysica acta*. 2013; 1832:1378–1383. [PubMed: 23517918]
21. Vale-Silva L, Ischer F, Leibundgut-Landmann S, Sanglard D. Gain-of-function mutations in PDR1, a regulator of antifungal drug resistance in *Candida glabrata*, control adherence to host cells. *Infect Immun*. 81:1709–1720. doi:IAI.00074-13 [pii] 10.1128/IAI.00074-13. [PubMed: 23460523]
22. Chen YL, et al. Convergent Evolution of Calcineurin Pathway Roles in Thermotolerance and Virulence in *Candida glabrata*. *G3 (Bethesda)*. 2:675–691. doi:10.1534/g3.112.002279 GGG_002279 [pii]. [PubMed: 22690377]
23. Farmakiotis D, Tarrand JJ, Kontoyiannis DP. Drug-Resistant *Candida glabrata* Infection in Cancer Patients. *Emerg Infect Dis*. 20:1833–1840. [PubMed: 25340258]

24. Pfaller MA, et al. Frequency of decreased susceptibility and resistance to echinocandins among fluconazole-resistant bloodstream isolates of *Candida glabrata*. *J Clin Microbiol*. 50:1199–1203. doi:JCM.06112-11 [pii] 10.1128/JCM.06112-11. [PubMed: 22278842]
25. Krissinel E, Henrick K. Secondary-structure matching (SSM), a new tool for fast protein structure alignment in three dimensions. *Acta Crystallogr D Biol Crystallogr*. 2004; 60:2256–2268. doi:S0907444904026460 [pii] 10.1107/S0907444904026460. [PubMed: 15572779]
26. Robert X, Gouet P. Deciphering key features in protein structures with the new ENDscript server. *Nucleic acids research*. 2014; 42:W320–W324. [PubMed: 24753421]
27. EUCAST definitive document EDef 7.1: method for the determination of broth dilution MICs of antifungal agents for fermentative yeasts. *Clin Microbiol Infect*. 2008; 14:398–405. doi:CLM1935 [pii] 10.1111/j.1469-0691.2007.01935.x. [PubMed: 18190574]

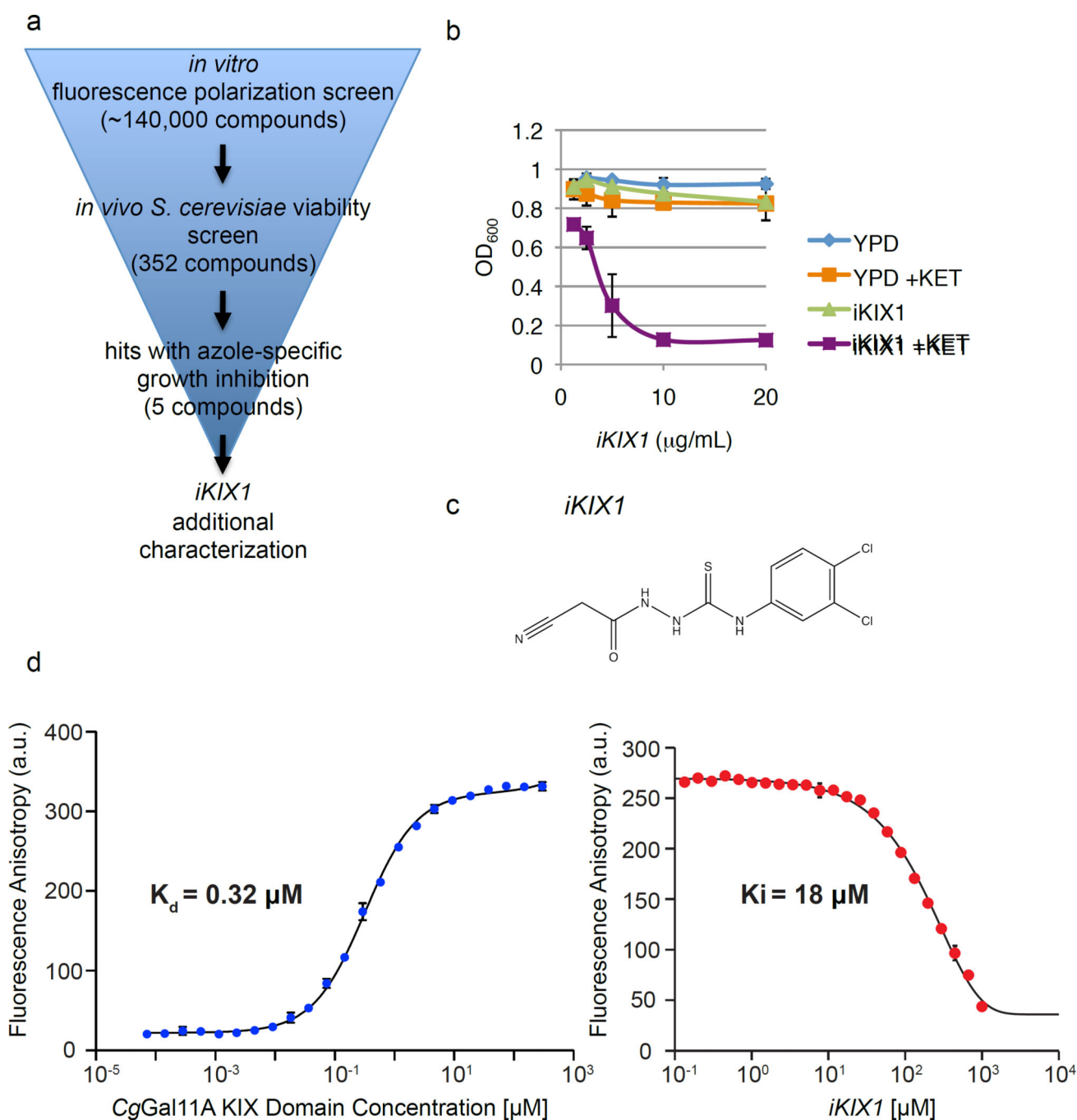


Figure 1. Discovery of inhibitors of the *CgGal11A* KIX-*CgPdr1AD* interaction interface

(a) Schematic of the screening process.

(b) *iKIX1* inhibits cell growth in a concentration-dependent manner in the presence of 5 μM ketoconazole (KET); error bars represent means \pm s.d. from duplicate plates.

(c) *iKIX1* structure.

(d) FP titration curve showing the interaction of *CgGal11A* KIX domain with *CgPdr1* AD30 fitted to a K_d of $319.7 \text{ nM} \pm 9.5 \text{ nM}$ (left). *iKIX1* competes out *CgPdr1* AD30 with an IC_{50} of $190.2 \text{ } \mu\text{M} \pm 4.1 \text{ } \mu\text{M}$ (right). The measured K_d and IC_{50} values were used to calculate an

apparent K_i of 18.1 μM for *iKIXI*. Data represent mean of two replicates and standard error from the fit is shown.

Author Manuscript

Author Manuscript

Author Manuscript

Author Manuscript

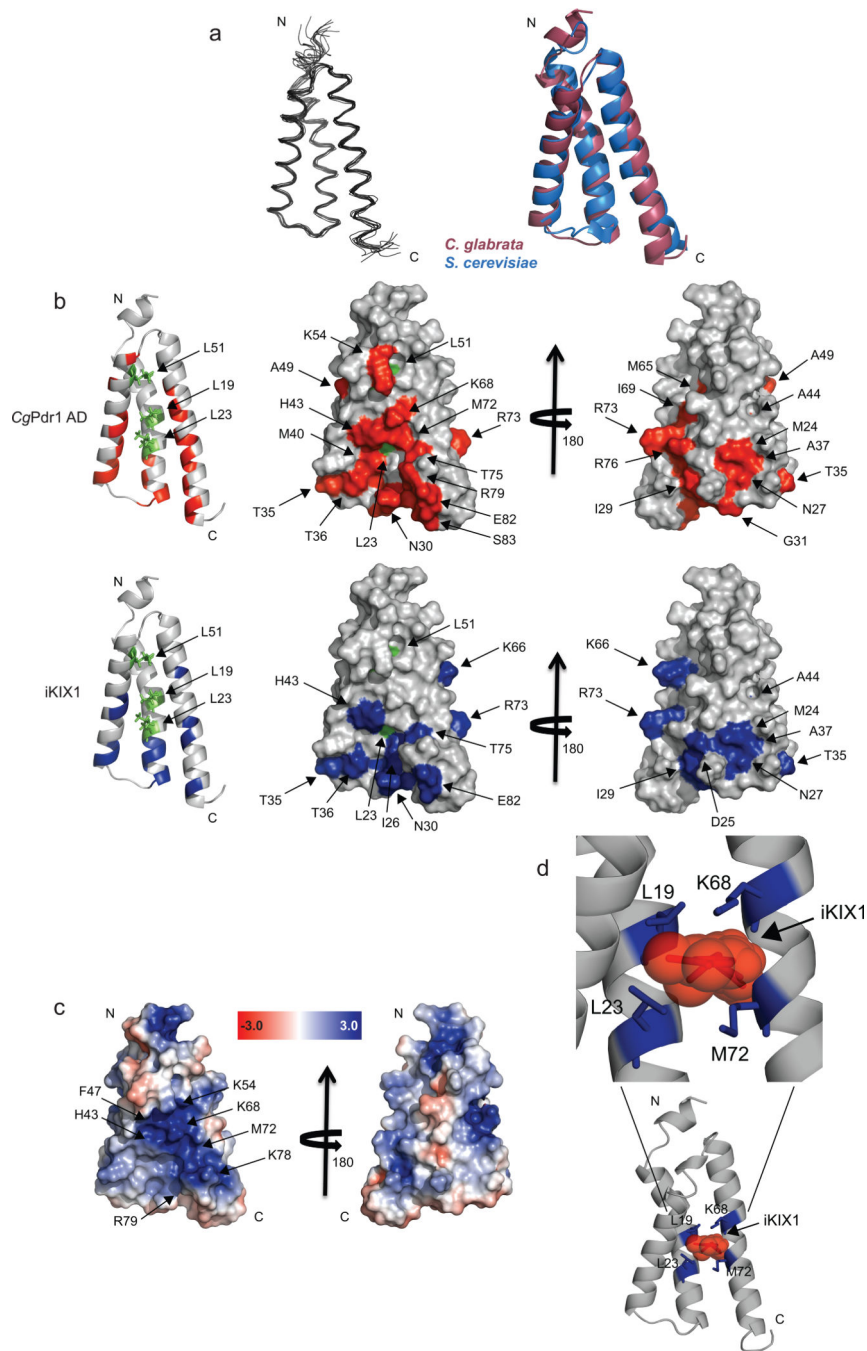


Figure 2. Elucidation of the *CgGal11A* KIX domain structure; *CgPdr1* AD and *iKIX1* bind to a similar interface on the *CgGal11A* KIX domain

(a) Backbone representation of the 10 lowest energy NMR structures of *CgGal11A* KIX domain; backbone RMSD ~ 0.7 Å, left. Overlay of *CgGal11A* (purple) and *S. cerevisiae* Gal11/Med15 (blue) KIX domains, with an overall RMSD of 2.0 Å²⁵, right.

(b) Chemical shift perturbations (CSPs) on the *CgGal11A* KIX domain in the presence of *CgPdr1* AD (red) or *iKIX1* (blue). Residues coloured in red or blue indicate a chemical shift perturbation greater than 2 s.d. Residues highlighted in green (L19, L23 and L51) represent significant CSPs in the side-chain methyl groups of an ILV labeled sample.

- (c) The *iKIX1* and *CgPdr1* AD target the hydrophobic groove on the *CgGal11A* KIX domain, which is surrounded by a basic patch. Residues H43, K54, K68, K78, R79, F47 and M72 present a positive electrostatic surface enclosing the binding interface.
- (d) *iKIX1* docked to the *CgGal11A* KIX domain. *iKIX1* is depicted as red sticks and spheres. Residues that experience significant methyl CSP upon addition of *iKIX1* are depicted as blue sticks.

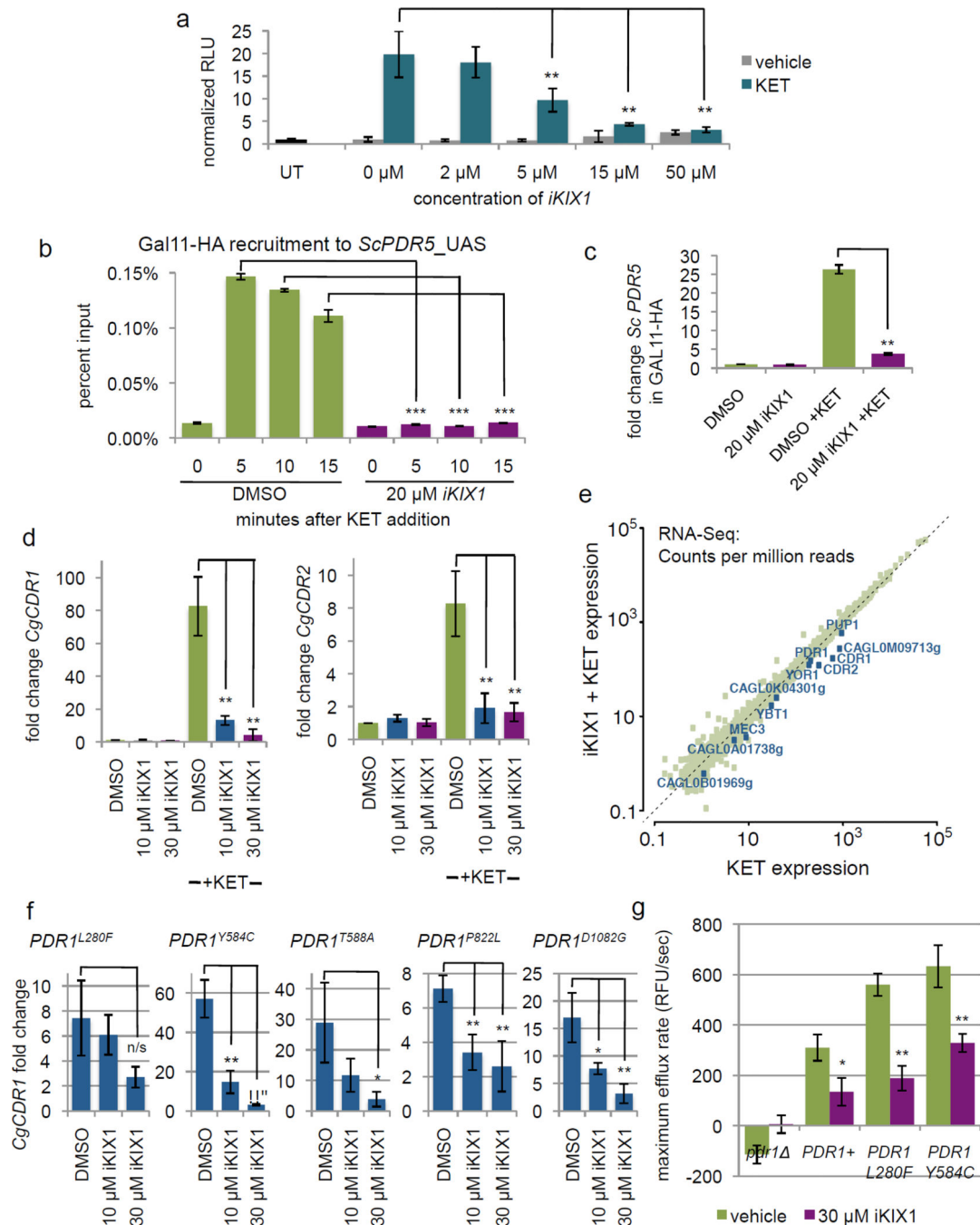


Figure 3. *iKIX1* blocks Gal11/Med15 recruitment and upregulation of Pdr1 target genes
 (a) *iKIX1* inhibits ketoconazole (KET)-induced upregulation of luciferase activity in a dose-responsive manner in a *Sc pdr1 pdr3* strain containing plasmid-borne *CgPDR1* and 3XPDR-luciferase. (UT): untreated control; ** P<0.001.
 (b,c) *iKIX1* prevents the ketoconazole (KET)-induced recruitment of Gal11/Med15/Mediator to the upstream activating sequences (UAS) of the PDRE-regulated promoter *ScPDR5* (B), and *ScPDR5* induction (C). Representative experiment from two biological replicates (ChIP DNA and RNA from same experiment) is shown. Error bars indicate s.d. of

technical replicates; *** $P < 0.00001$, ** $P < 0.0005$, and * $P < 0.01$ by two-tailed Student's t-test.

(d) *iKIX1* inhibits ketoconazole (KET)-induced transcriptional upregulation of *CgCDR1* and *CgCDR2* in a *CgPDR1* wild-type strain (SFY114). ** $P < 0.005$.

(e) RNA-Seq analysis of a *C. glabrata* SFY114 (*PDR1* wild-type) strain pre-treated with *iKIX1* or vehicle alone then induced with ketoconazole (*iKIX1* + KET and KET, respectively).

(f) *iKIX1* inhibits xenobiotic-induced *CgPdr1* transcription in *CgPdr1* gain-of-function mutants (amino acid changes indicated). Samples shown were induced with ketoconazole. * $P < 0.05$ and ** $P < 0.01$ as compared to DMSO + ketoconazole control.

(g) *iKIX1* inhibits rhodamine 6G efflux in *C. glabrata* as compared to vehicle control. * $P < 0.05$, ** $P < 0.005$ as compared to DMSO + ketoconazole control.

(a,d,e,f,g) Data represent the means of three biological replicates. Two-tailed student's t-test used to determine P values; error bars represent means \pm standard deviation.

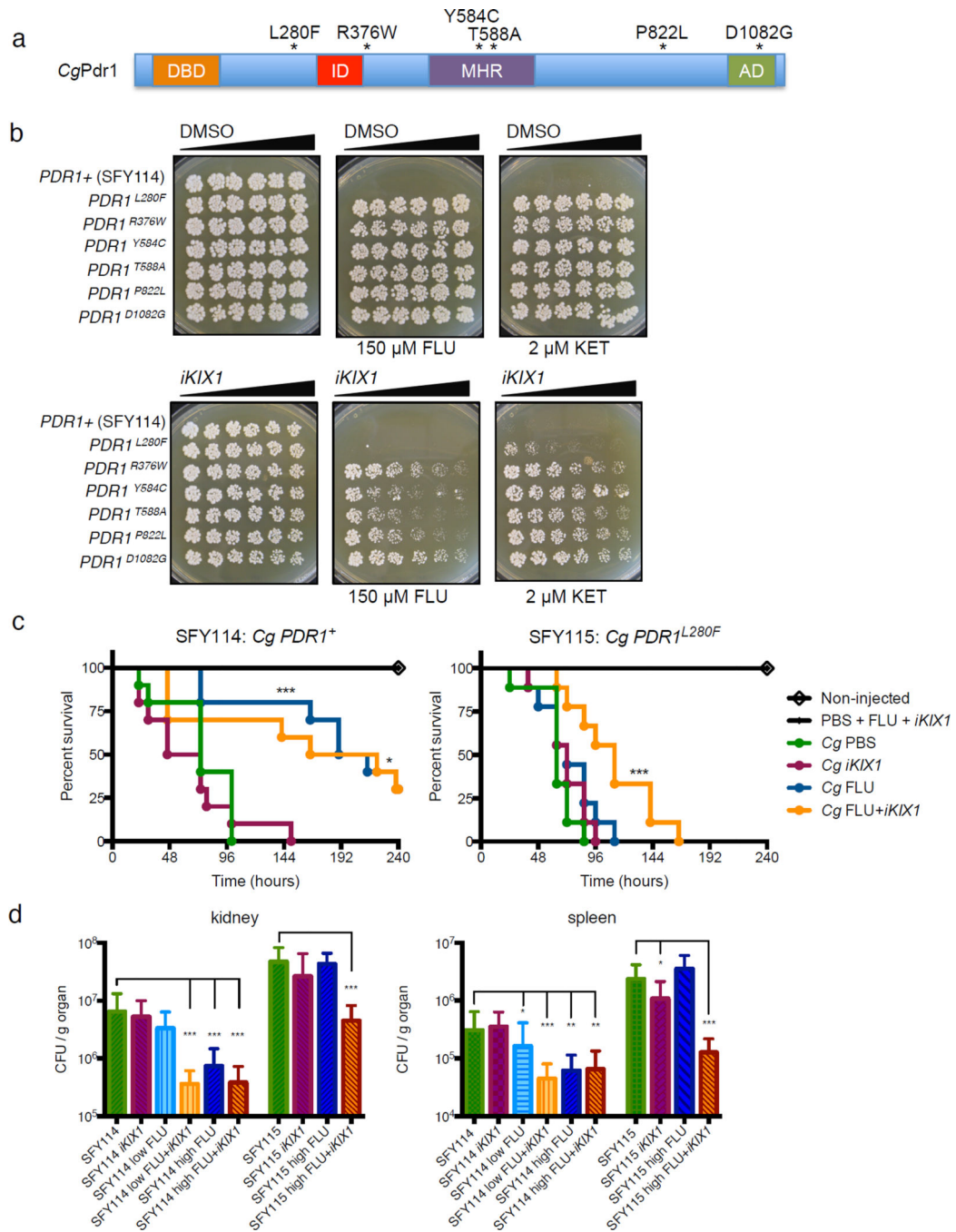


Figure 4. *iKIX1* as a co-therapeutic in models of *C. glabrata* disseminated disease

(a) Schematic showing *CgPdr1* gain-of-function alterations in relation to putative functional domains. DBD: DNA-binding domain, ID: inhibitory domain, MHR: middle homology region, AD: activation domain.

(b) *iKIX1* restores the efficacy of azoles towards *CgPDR1* gain-of-function mutants. Plates contained increasing concentrations of vehicle control (DMSO) or *iKIX1* to 150 μ M in the absence or presence of fluconazole (FLU) or ketoconazole (KET).

(c) *iKIX1* in combination with fluconazole but not fluconazole alone significantly extended survival of *G. mellonella* larvae injected with *CgPDR1^{L280F}* (SFY115, n=9). For SFY114, n=10. * P<0.05, *** P<0.001 as compared to PBS vehicle control. Statistical differences measured using a log-rank (Mantel-Cox) test.

(d) *iKIX1* combination treatment with 25 mg/kg fluconazole (low FLU) reduces fungal tissue burden in the kidney or spleen of mice injected with *CgPDR1* wild-type (SFY114); *iKIX1* in combination with 100 mg/kg fluconazole (high FLU) reduces fungal tissue burden in the kidney or spleen of mice injected with *CgPDR1^{L280F}* (SFY115). N=5 mice for each treatment condition; * P<0.05, ** P< 0.005 and *** P< 0.0001 as compared to no treatment. Statistical differences measured using a Wilcoxon rank-sum test; error bars represent means +/- standard deviation.